Acta Pharmacologica Sinica (2017) 38: 764–781
www.nature.com/aps

*Open*

Review

# Conjugated polymer nanomaterials for theranostics

Cheng-gen QIAN[1, 2, #], Yu-lei CHEN[1, #], Pei-jian FENG[1], Xuan-zhong XIAO[1], Mei DONG[1], Ji-cheng YU[2, 3], Quan-yin HU[2, 3], Qun-dong SHEN[1, *], Zhen GU[2, 3, 4, *]

*[1]Department of Polymer Science and Engineering and Key Laboratory of High Performance Polymer Materials and Technology of MOE, School of Chemistry and Chemical Engineering, Nanjing University, Nanjing 210023, China; [2]Joint Department of Biomedical Engineering, University of North Carolina at Chapel Hill and North Carolina State University, Raleigh, NC 27695, USA; [3]Center for Nanotechnology in Drug Delivery and Division of Pharmacoengineering and Molecular Pharmaceutics, Eshelman School of Pharmacy, University of North Carolina at Chapel Hill, Chapel Hill, NC 27599, USA; [4]Department of Medicine, University of North Carolina School of Medicine, Chapel Hill, NC 27599, USA*

**Abstract**

Conjugated polymer nanomaterials (CPNs), as optically and electronically active materials, hold promise for biomedical imaging and drug delivery applications. This review highlights the recent advances in the utilization of CPNs in theranostics. Specifically, CPN-based *in vivo* imaging techniques, including near-infrared (NIR) imaging, two-photon (TP) imaging, photoacoustic (PA) imaging, and multimodal (MM) imaging, are introduced. Then, CPN-based photodynamic therapy (PDT) and photothermal therapy (PTT) are surveyed. A variety of stimuli-responsive CPN systems for drug delivery are also summarized, and the promising trends and translational challenges are discussed.

**Keywords:** conjugated polymer; theranostics; biomedical imaging; photodynamic therapy; photothermal therapy; stimuli-responsive drug delivery

*Acta Pharmacologica Sinica* (2017) 38: 764–781; doi: 10.1038/aps.2017.42; published online 22 May 2017

## Introduction

Conjugated polymers (CPs) are a special class of macromolecules with large π-conjugated backbones. Owing to their highly electron-delocalized structures and efficient coupling between optoelectronic segments, CPs have a particular capability to absorb and emit light energy, which can be effectively converted to fluorescence, heat, and other energies[1–4]. Conjugated polymer nanomaterials[5–11] (CPNs), as both optically and electronically active materials, have been shown to be promising theranostic agents[12–18]. Owing to their excellent light-harvesting and light-amplifying properties, CPNs have been applied to both *in vitro* and *in vivo* fluorescence imaging to achieve real-time diagnostics[19–24]. However, conventional fluorescence imaging suffers from general limitations such as poor spatial resolution and shallow tissue penetration[25–27]. Recently, with advancements in optical imaging techniques and materials science, a variety of powerful *in vivo* imaging methodologies have emerged[28]. Among them, near-infrared (NIR) imaging[29, 30], two-photon (TP) imaging[31, 32], photoacoustic (PA) imaging[27, 33], and multimodal (MM) imaging[34–36] can provide deep tissue penetration and high spatial resolution, which offer new opportunities for the innovative application of CPNs in theranostics.

In addition to directly providing diagnostic signals, CPNs are also involved in minimally invasive therapeutic techniques such as photodynamic therapy (PDT)[37–40] and photothermal therapy (PTT)[41–44]. PDT is an effective noninvasive therapeutic technique used in clinical cancer treatment. This technique utilizes photosensitizers to transfer energy from light to oxygen molecules and generate cytotoxic reactive oxygen species (ROS). By using light-absorbing agents, PTT converts the light radiation into thermal (vibrational) energy to ablate cancer cells. PTT has emerged as a next generation of noninvasive methodology for cancer therapy. In addition, the convergence of drug delivery systems with PDT or PTT for combination therapy has also been achieved for enhanced therapeutic efficacy[45–49]. In this review, we will focus on CPN-based theranostic (a combination of diagnostics and therapy) systems for imaging, PDT and PTT, as well as stimuli-responsive drug delivery (Figure 1). Future opportunities and challenges will also be discussed.

# These authors contributed equally to this work.
*To whom correspondence should be addressed.
E-mail zgu@email.unc.edu (Zhen GU);
qdshen@nju.edu.cn (Qun-dong SHEN)
Received 2016-12-12 Accepted 2017-03-02

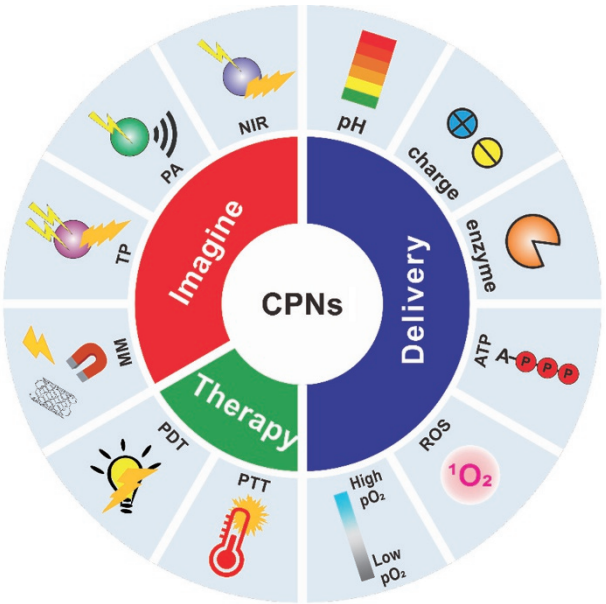


**Figure 1.** Schematic of utilizing conjugated polymer nanomaterials (CPNs) for theranostics.

### CPNs for biomedical imaging

Fluorescence microscopy techniques play a crucial role in biomedical imaging[50]. Owing to their highly efficient light harvesting, multiple emissive wavelengths, ease of modification, excellent photostability and low cytotoxicity, CPNs have recently attracted considerable attention in biological fluorescence imaging and sensing[18, 51, 52]. Most current optical theranostic techniques rely on emitted photons as the signal readout and thus inevitably suffer from the drawbacks of autofluorescence background of the tissue and limited capability of light penetration, which may compromise the diagnostic accuracy[25, 27]. To meet the requirement of *in vivo* applications, a variety of new CPs and relevant imaging techniques, including NIR imaging, TP imaging, PA imaging and MM imaging, have been exploited.

Fluorescence imaging in the second near-infrared (NIR II, 1.0–1.7 μm) region has recently attracted significant attention owing to the advantages in imaging in the visible (400–750 nm) and the conventional near-infrared (NIR 1750–900 nm) regions[53–55]. Photons in the NIR-II region can provide high spatial resolution at deep tissue penetration depths owing to the reduced scattering of long-wavelength photons[56]. For example, Hong and co-workers synthesized a series of the CPs with tunable emission wavelengths in the NIR-II region through donor-acceptor alternating copolymerization[57] (Figure 2A). They functionalized the polymer core non-covalently with a PEGylated surfactant as the shell, which afforded water

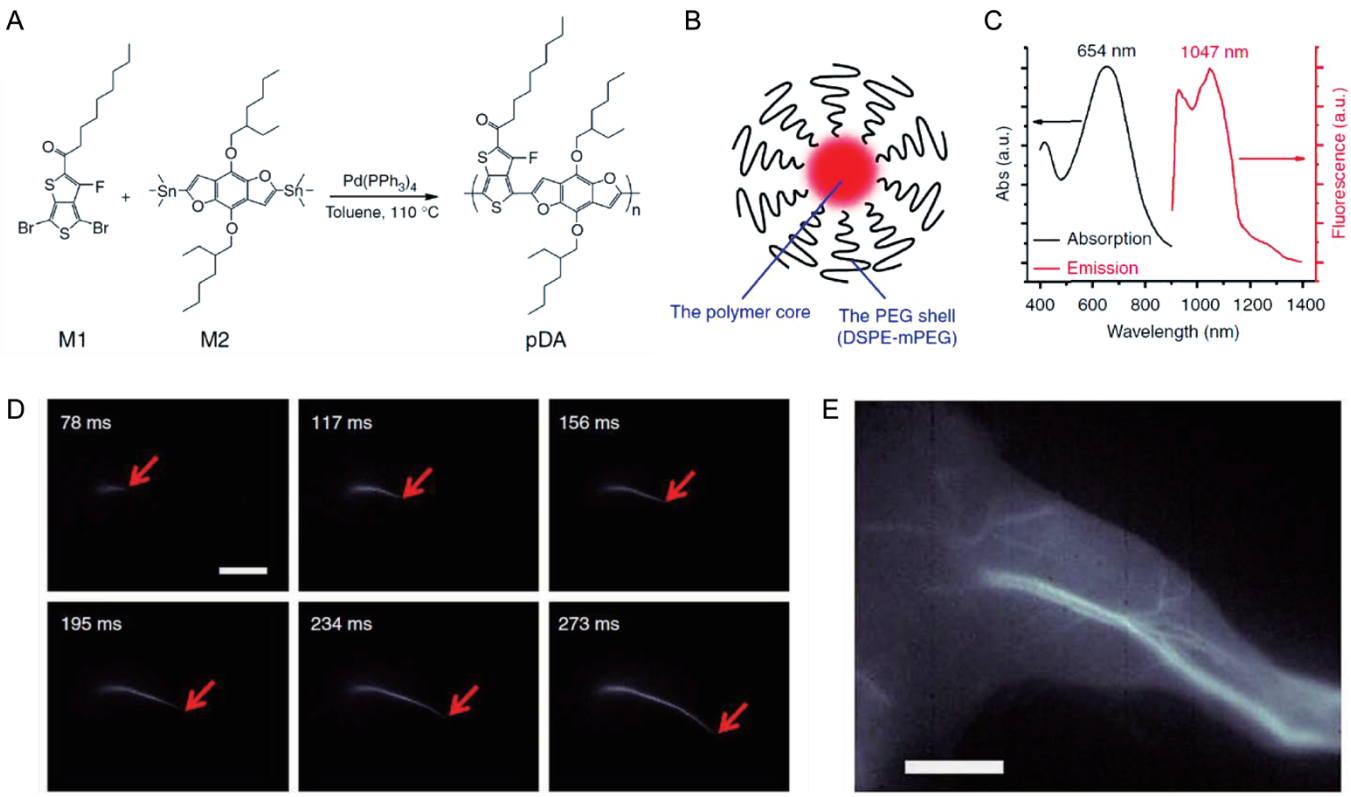


**Figure 2.** (A) Synthesis of the conjugated polymer pDA. (B) The nanoparticle (pDA-PEG) with a hydrophobic conjugated polymer core and a hydrophilic PEG shell. (C) Absorption and emission spectra of pDA-PEG. (D) Ultrafast second near-infrared (NIR-II) imaging of arterial blood flow. (E) The NIR-II fluorescence image of the same mouse hindlimb after full perfusion of pDA-PEG containing blood into the hindlimb. The scale bars are 5 mm. Reproduced with permission from Ref[57].

solubility and biocompatibility (Figure 2B and 2C). The NIR-II fluorescent probe exhibited a quantum yield of 1.7% and thus allowed for *in vivo* and deep-tissue imaging. Ultrafast imaging of mouse arterial blood flow with an unprecedented imaging speed of more than 25 frames per second was achieved (Figure 2D and 2E). The fluorophores improved the penetration depth and enabled dynamic imaging with great spatiotemporal resolution, thus demonstrating that NIR-II fluorescence systems are suitable for clinical applications. Most recently, the same group developed a novel NIR-II fluorescent probe to investigate cerebrovascular injury in a mouse traumatic brain injury (TBI) model[58]. With the aid of an *in vivo* NIR-II imaging system, they could directly visualize dynamic vascular changes in a mouse TBI model, including initial transient hypoperfusion that was resolved as fluorophore leakage and accumulation caused by damage to the cerebrovasculature.

TP excitation microscopy is a noninvasive imaging technology for living cells and tissues with excellent spatial resolution, deep-tissue penetration, less interference from autofluorescence, and minimal photodamage to living biosubstrates[31, 59, 60]. Distinguished from the conventional one-photon excitation microscopy, TP excitation arises from the simultaneous absorption of two photons in a single quantitized event. Thus, the large two-photon absorption (TPA) cross sections and high emission quantum yields of fluorophores are the key requirements for TP imaging[61, 62]. CPs have highly delocalized π-conjugated backbones and display large one- and two-photon absorption coefficients, high fluorescence quantum yields, and good photostability, which make them promising for TP imaging[63, 64]. In addition, the wavelength of excitation light for TP imaging is usually in the NIR regions (700–1000 nm), where water and blood are nearly transparent and non-scattering[65, 66].

Li and co-workers reported the use of red-emitting dye-doped CP nanoparticles for TP cancer cell imaging[67]. Conjugated polymer (PFV) and red-emitting dye magnesium phthalocyanine (MgPc) were encapsulated in polyoxyethylene nonylphenylether (CO-520) to form nanoparticles with the excitation wavelength of 800 nm (Figure 3A). In these nanoparticles, PFV with large TPA cross sections was chosen as a TP light-harvesting material, and MgPc with high emission quantum yields was chosen as the energy acceptor and red-emitting material (Figure 3B). The TP-based fluorescence resonance energy transfer (FRET) from the CPs to the dyes could be utilized to prepare NIR excited red-emitting materials for deep-tissue live-cell imaging; it can be applied to most CPs with light absorption in the visible range. The TP excitation fluorescence of MgPc in MgPc/PFV NPs was enhanced by up to 53 times. These nanoparticles displayed excellent biocompatibility (Figure 3C). In the TP imaging of HepG2 cancer cells, the cytoplasm could be clearly distinguished. Additionally, the cell morphology was readily discerned by the strong fluorescence (Figure 3D).

PA tomography is an emerging technology that overcomes

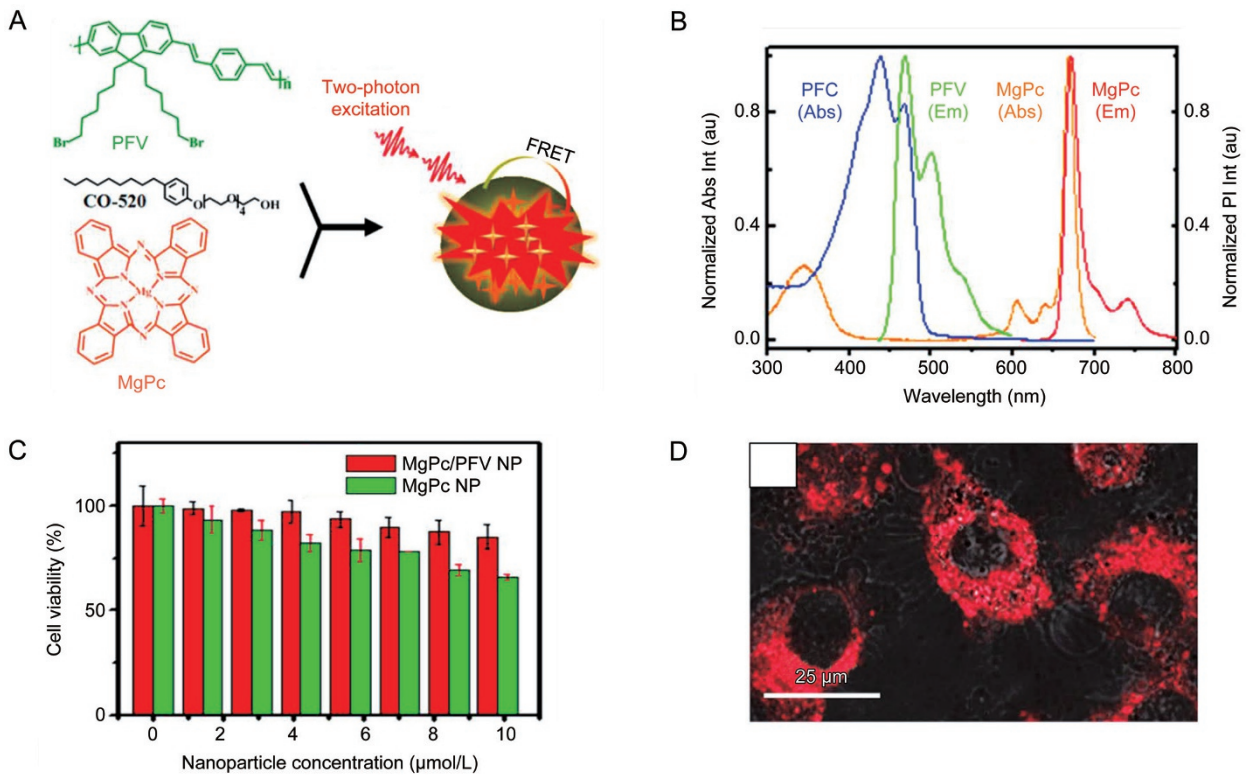


**Figure 3.** (A) Schematic preparation procedures of MgPc/PFV NPs. (B) Normalized absorption and emission spectra of PFV NPs and MgPc NPs. (C) *In vitro* cytotoxicity of HepG2 cancer cells treated with MgPc/PFV NPs and MgPc NPs containing the same amount of MgPc for 8 h. (D) TP fluorescent image of HepG2 cancer cells treated with MgPc/PFV NPs. The scale bar is 25 μm. Reproduced with permission from Ref[67].

the multiple scattering of optical photons in biological tissues by making use of the photoacoustic effect. Light absorption by photoacoustic contrast agents creates a thermally induced pressure jump that launches ultrasonic waves, which are received by acoustic detectors to form images[27]. PA imaging exceeds the optical diffusion limit via detection of phonons, instead of photons, upon light excitation[68–70]. PA imaging has great potential for the visualization of physiology and pathology at the molecular level because of the deep tissue penetration and excellent spatial resolution. Pu and co-workers reported NIR-absorbing semiconducting polymer nanoparticles (SPNs) as an efficient and stable nanoplatform to generate ultrasound wave for *in vivo* photoacoustic molecular imaging[71]. Two polymer derivatives with strong absorption within the NIR region were chosen (Figure 4A–4C). These nanoparticles produced a stronger signal than the commonly used single-walled carbon nanotubes and gold nanorods, permitting whole-body lymph node photoacoustic mapping in living mice with low-volume injections (Figure 4D). Furthermore, they coupled the nanoparticles to a cyanine dye derivative (IR775S) that was sensitive to ROS-mediated oxidation to obtain a probe for ROS imaging. This example of ROS imaging demonstrated that the conjugated polymer nanoparticles possessed high structural flexibility and could be an ideal nanoplatform for photoacoustic molecular probes. The PA signal comes mainly from photothermal conversion. Thereby, the criterion for selecting PA imaging probes is consistent with that for PTT. This similarity makes PA and PTT an ideal pair to be seamlessly and synergistically combined into theranostics. Lyu and co-workers further confirmed that the PA intensity of SPNs was proportional to their photothermal conversion efficiency and thus envisioned the utility of SPNs in cancer treatment[72]. Recently, Fan *et al* demonstrated perylene-diimide-based nanoparticles as highly efficient photoacoustic agents for deep brain tumor imaging[73].

Compared to single modality, MM imaging can satisfy the increasing requirements in advanced biotechnology. Sun and co-workers developed conjugated polymer-labeled magnetic nanoparticles using a layer-by-layer assembly technique for dual-modal fluorescent-magnetic resonance imaging[74, 75] (Figure 5A and 5B). The fluorescent-magnetic nanoparticles were used for both tracking the cellular uptake of nanomaterials and controlling the cellular uptake by an external magnetic field. The results demonstrated a higher uptake ability of the fluorescence-labeled magnetic nanoparticles with the aid of a magnetic field. Subsequently, Li and co-workers synthesized

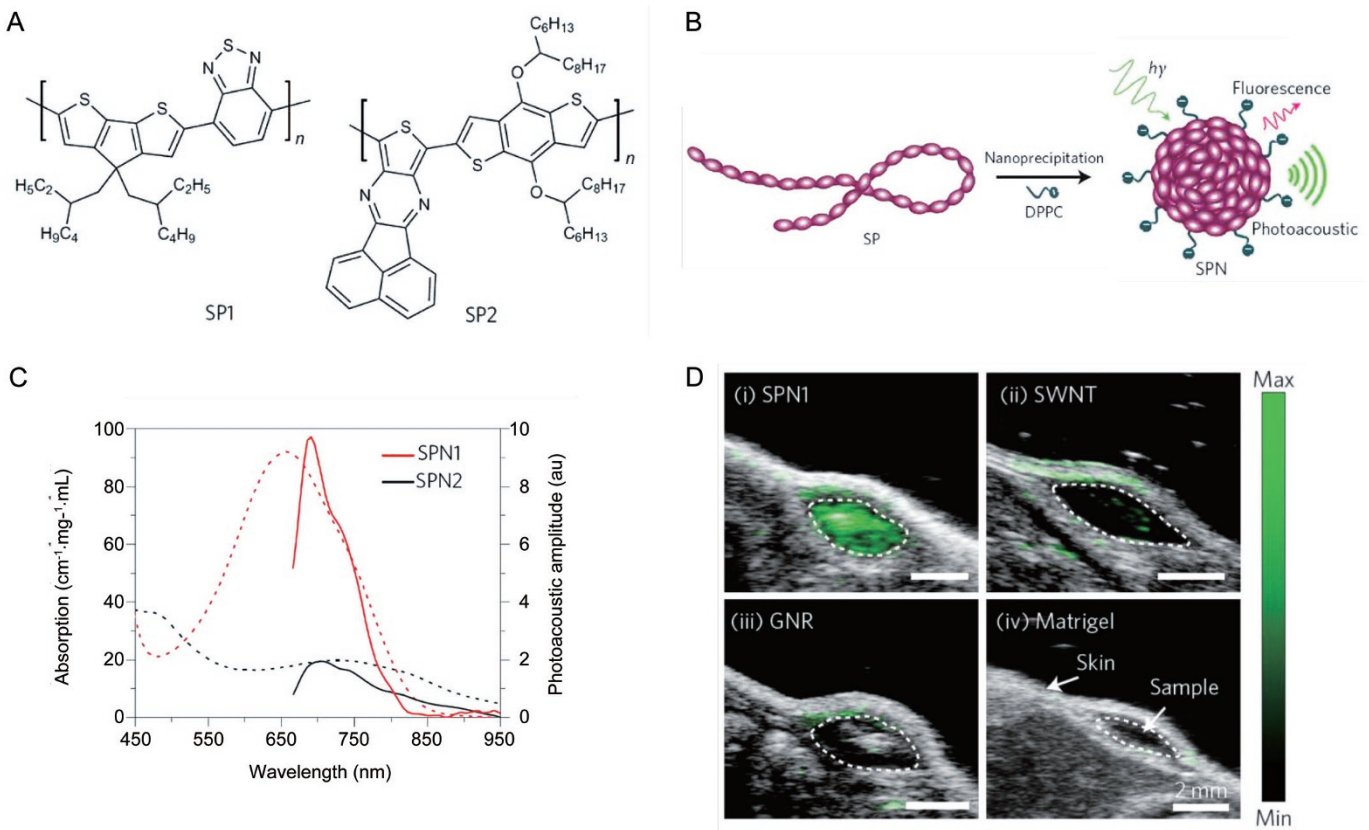


**Figure 4.** (A) Molecular structures of conjugated polymer SP1 and SP2. (B) Schematic of the preparation of the semiconducting polymer nanoparticles (SPN). (C) Ultraviolet-visible absorption (dashed lines) and photoacoustic (solid lines) spectra of SPNs. (D) Comparison of photoacoustic properties of SPN1 with single-walled carbon nanotubes (SWNTs) and gold nanorods (GNRs). Photoacoustic/ultrasound co-registered images of the nanoparticle-matrigel inclusions in the mice. The images represent transverse slices through the subcutaneous inclusions (dotted circles). The scale bars are 2 mm. Reproduced with permission from Ref[71].

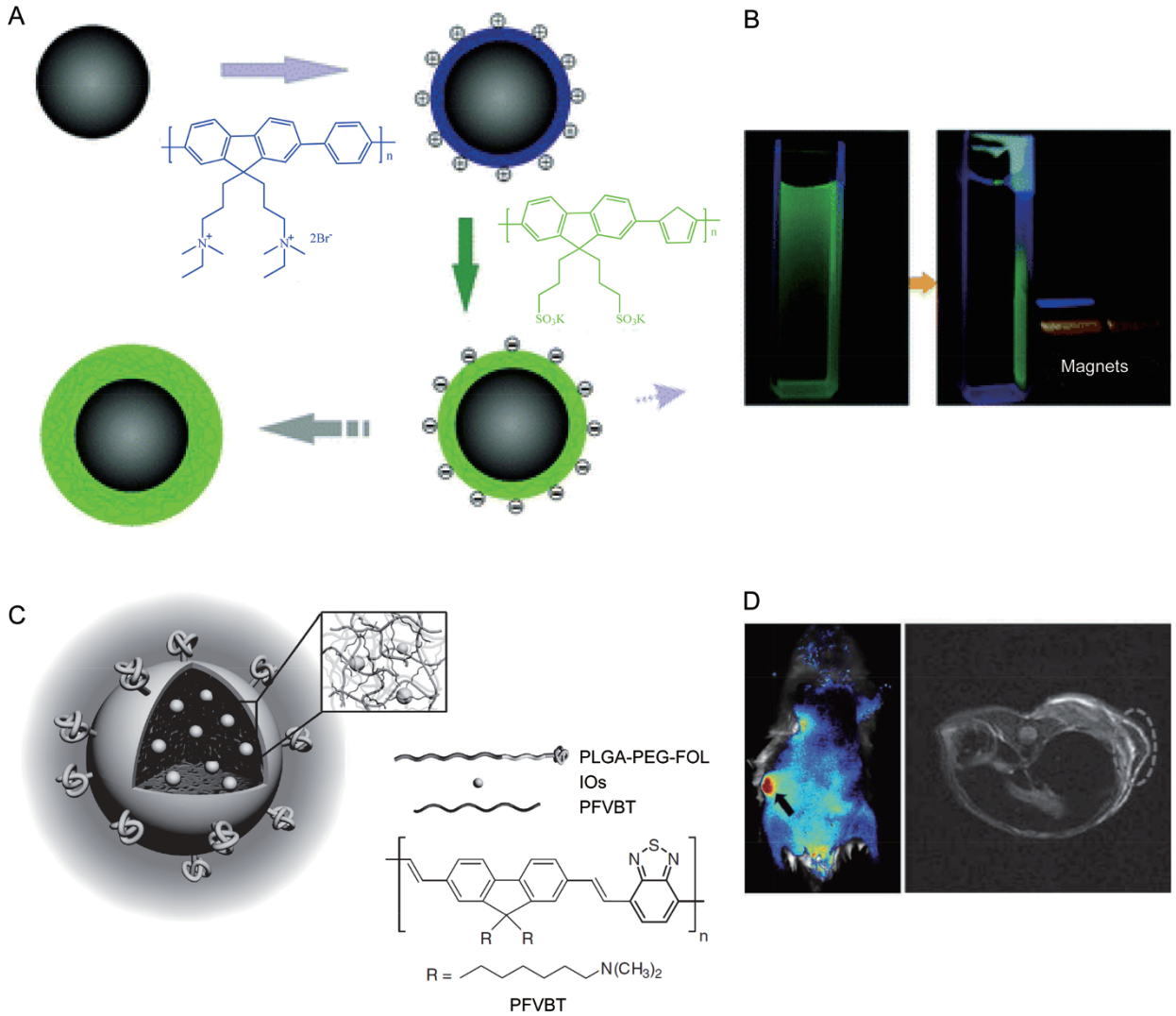


**Figure 5.** (A) Electrostatic adsorption of the CPs on surfaces of the magnetic nanoparticles to afford magnetic-fluorescent nanoparticles (MF NPs) by layer-by-layer assembly. (B) Images of MF NPs under UV light irradiation without (left) and with magnets (right). (C) Schematic of the conjugated polymer based MF NPs and the chemical structure of conjugated polymer PFVBT. (D) *In vivo* fluorescence images (left) and magnetic resonance images (right) of the mouse treated with MF NPs. Reproduced with permission from Ref[20, 74].

the conjugated polymer with emissions in the far-red/near-infrared region[20]. They fabricated the fluorescent magnetic nanoparticles by co-encapsulating the conjugated polymer and lipid-coated iron oxides (IOs) with a mixture of poly(ethylene glycol)-folate and PLGA for *in vivo* MM imaging (Figure 5C and 5D).

Liu *et al* reported a fluorescence-Raman dual-imaging method for intercellular tracking[76]. They fabricated a CPE-cMWNT nanosystem with electrostatic adsorption between oppositely charged carbon nanotubes (cMWNTs) and conjugated polyelectrolytes (CPEs) (Figure 6). The red fluorescent cationic CPE (TBtPFN) was coated on the negatively charged surface of cMWNTs to form TBtPFN/cMWNT nanocomposites and these were then coated with green fluorescent anionic CPE (BtPFS) as a second layer to form the dual-color fluorescence-labeled carbon nanotubes (BtPFS/TBtPFN/cMWNTs). Fluorescence-Raman dual-imaging showed the characteristic red and green fluorescence of TBtPFN and BtPFS, respectively. Meanwhile, carbon nanotubes produced robust and resonance-enhanced Raman bands owing to their diameter and electronic structure, which could be used for Raman mapping of CPE-cMWNT nanocomposites distribution in Bel-7402 cells. The high flexibility of electrostatic assembly facilitates their interaction with various biological substances for drug delivery and diagnostic imaging.

Fan and co-workers reported a novel melanin-based MM imaging nanoplatform for PA imaging, positron emission tomography (PET) and magnetic resonance imaging (MRI)[77] (Figure 7). Melanin is a naturally occurring pigment, and has been pursued as a biomarker for melanoma imaging[78, 79]. The authors prepared ultra-small melanin nanoparticles (MNPs) from melanin granules and further used these water-soluble

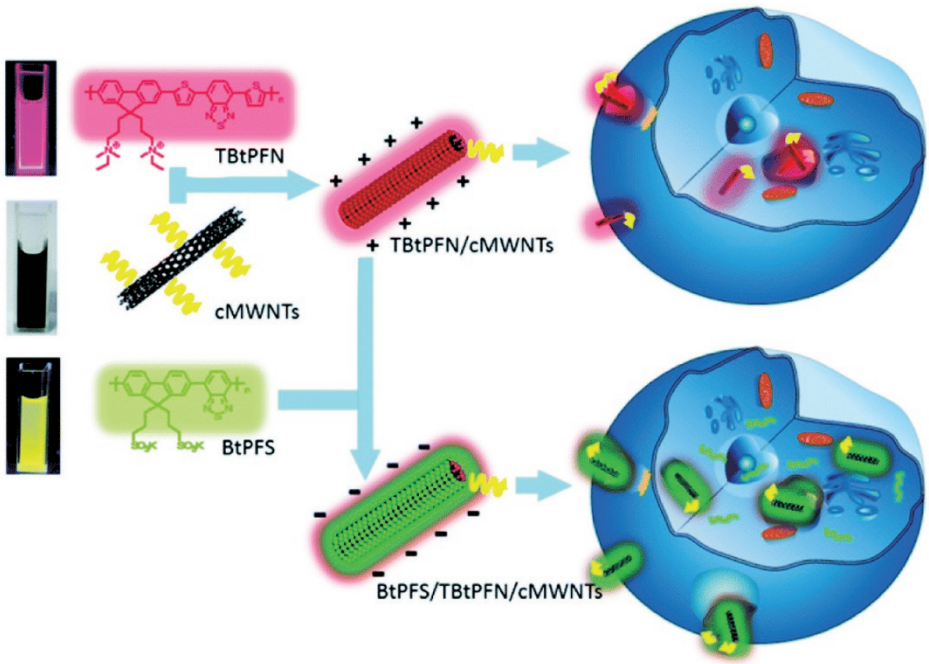


**Figure 6.** Schematic of the preparation of the charged carbon nanotubes (cMWNTs) and the CPE-cMWNT nanocomposites of the conjugated polyelectrolytes (CPEs) with cMWNTs. Reproduced with permission from Ref[76].

MNPs as a good endogenous nanoplatform for tumor multimodality imaging. The MNPs showed unique the photoacoustic property and natural binding ability with metal ions (such as $^{64}Cu^{2+}$, $Fe^{3+}$) (Figure 7A). *In vivo* imaging results showed that MNPs not only serve as a photoacoustic contrast agent for PA imaging but also actively chelate metal ions for PET and MRI (Figure 7B–7E). Recently, the same group developed an MNP-based drug delivery system for multimodality-imaging guided chemotherapy[80]. This work provided an efficient single nanosystem for tumor therapy and clinical translation.

In addition, CPN-based MM imaging systems as biosensing fluorescent probes have attracted considerable attention in recent years. For example, Wang and co-workers developed an optical nanoruler system for label-free protein detection based on the distance-dependent metal-enhanced fluorescence (MEF) effect[81]. The detection mechanism is shown in Figure 8. A water-soluble cationic conjugated polymer (PFVCN) was selected as the fluorescence probe. Quartz slides with silver prisms nanostructures were used to produce the MEF effect. After bioconjugation of the antibody onto the surface and the antibody-antigen recognition, the distance between surface-bound PFVCN and bottom Ag nanostructure changes, leading to the MEF effect. Thus, changes in the fluorescent signal of PFVCN represented the binding event of the specific protein. Most recently, the same group constructed a hybrid probe of graphene oxide and cationic conjugated polymer for calmodulin sensing based on a fluorescence resonance energy transfer (FRET) strategy[82]. The presence of graphene oxide played an important role in sensing calcium ions by FRET between the conjugated polymer and calmodulin.

### CPNs for phototherapy

In addition to biological imaging, CPNs have also been explored as agents for phototherapy[17, 83]. CPNs can sensitize oxygen molecules under light irradiation to produce ROS and thus be used in PDT[84–86]. Moreover, CPNs with strong NIR absorption and high heat conversion efficiency have potential as a new generation of agents for PTT[87]. PDT and PTT hold great promise for non-invasive cancer treatment, and CPN-based image-guided therapy is a burgeoning area of research[87–93]. In addition, several new therapeutic approaches based on the mechanism of PDT and PTT have also been investigated. We will introduce the most recent advances in this section.

Most of the CPs with short-lifetime fluorescent emission suffer interference from background fluorescence[18]. Thus, developing novel CPNs with high utilization efficiency remains challenging. Shi and co-workers developed novel phosphorescent conjugated polymer dots (Pdots) containing Ir(III) complexes for optical oxygen sensing and photodynamic cancer therapy[23]. The long emission lifetime of the phosphorescent Ir(III) complexes can offer an effective way to eliminate the interferences from autofluorescence[94, 95]. The Pdots were composed of polyfluorene units and phosphorescent Ir(III) complexes in the main polymer chains via Suzuki coupling reaction and offered an efficient energy transfer from the conjugated polymer main chain to the phosphorescent Ir(III) complex (Figure 9A). The Pdots possessed fine photostability, biocompatibility, and ultrasmall size (<10 nm) (Figure 9B), which made the cellular uptake of the Pdots easier. The Pdots with phosphorescent Ir(III) complexes could serve

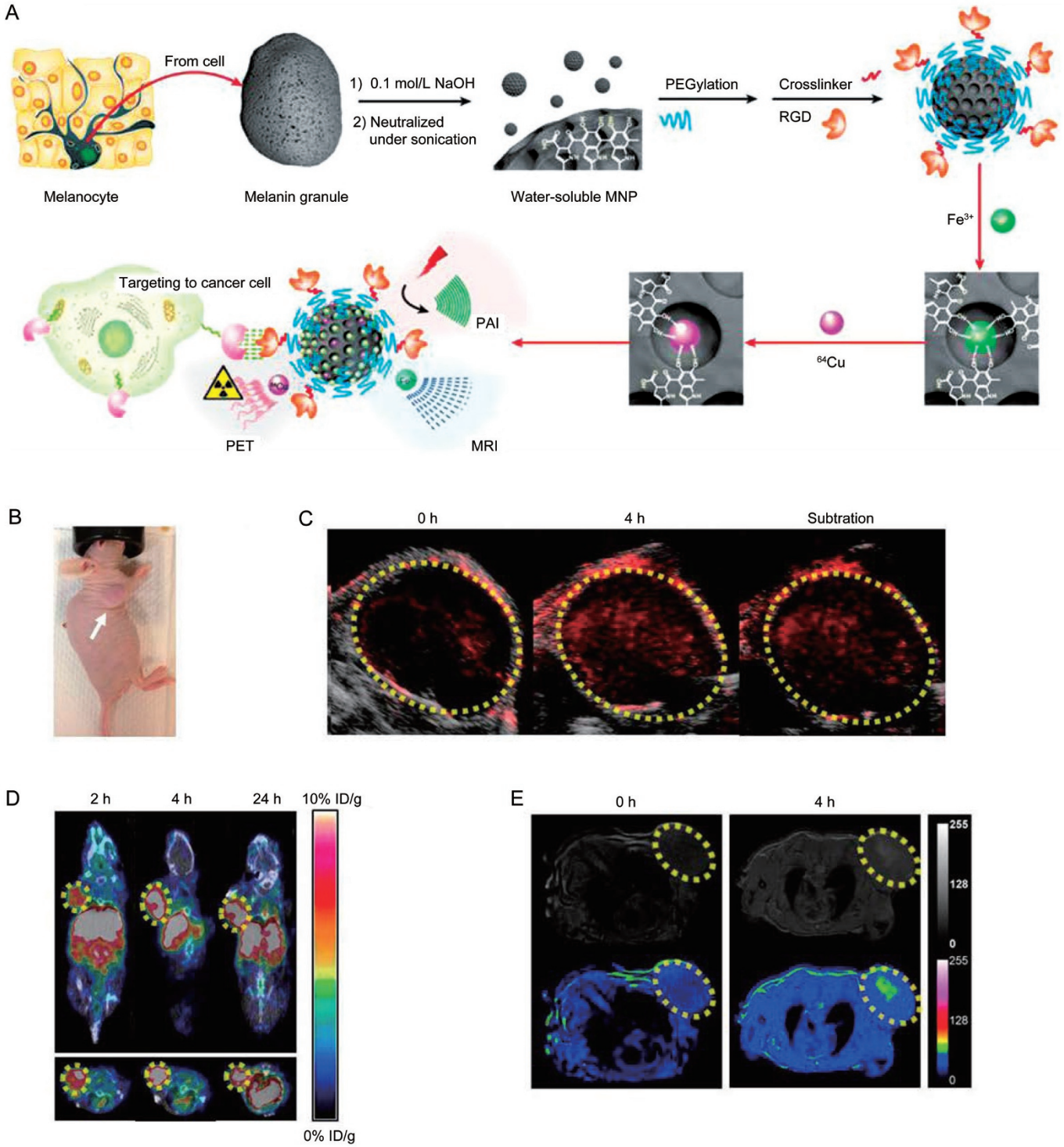


**Figure 7.** (A) Schematic illustration of the multimodal (MM) imaging melanin nanoplatform (MMPs). (B) Photographic images of U87MG tumor bearing mice. *In vivo* multimodality imaging of U87MG tumor (region enveloped by yellow dotted line) bearing mice after tail vein injection of $^{64}$Cu-Fe-RGD-PEG-MNP, including (C) photoacoustic (PA) imaging, (D) magnetic resonance imaging (MRI), and positron emission tomography (PET), respectively. Reproduced with permission from Ref[77].

as an optical probe for monitoring oxygen due to the triplet state that can quench the triplet phosphorescence. Meanwhile, the energy transfer enables the $^1O_2$ generation, causing effective apoptosis and death of cancer cells in the photodynamic therapy process (Figure 9C). This study provided a strategy for designing multifunctional nanoplatforms in tumor hypoxia

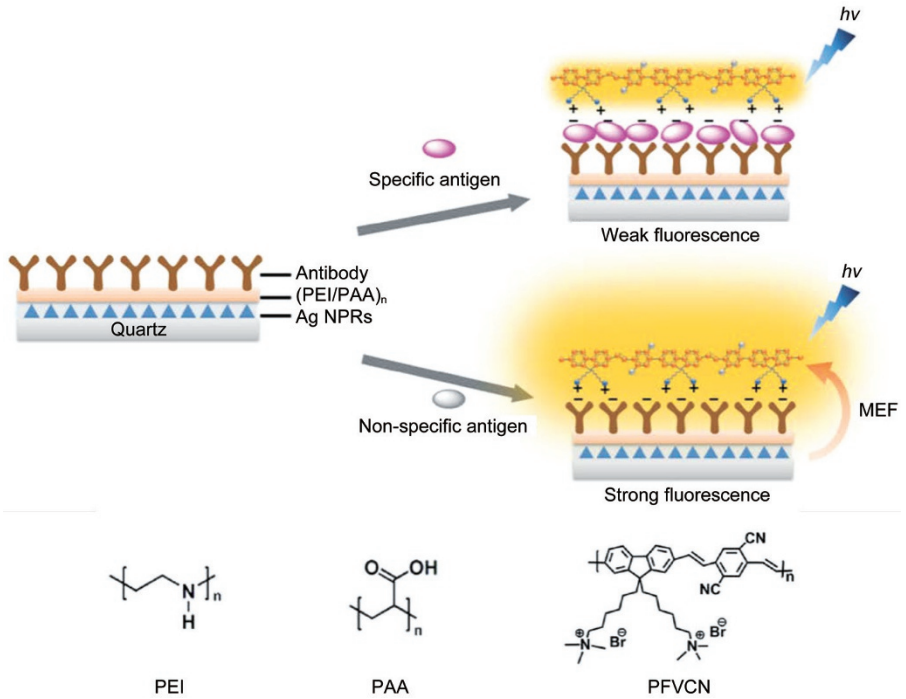


**Figure 8.** Schematic illustration of the structure and the mechanism of nano-rule detection platform for specific antigen detection assay. Reproduced with permission from Ref[81].

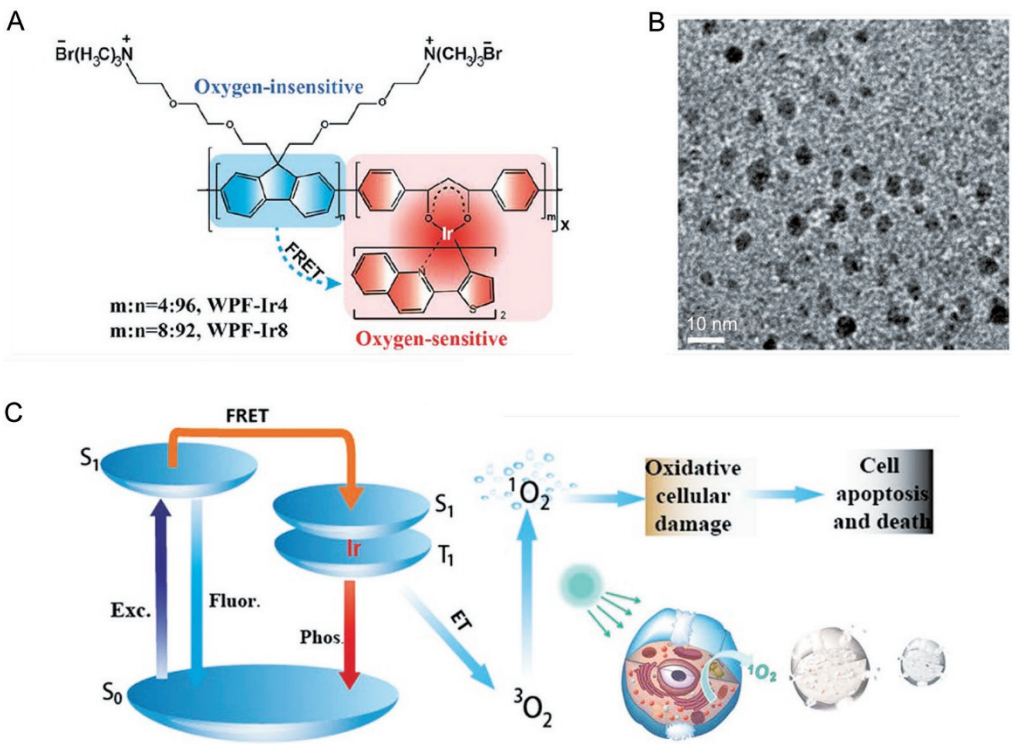


**Figure 9.** (A) Chemical structures of phosphorescent conjugated polymer with the Ir(III) complexes (Pdots). (B) High resolution transmission electron microscopy (HR-TEM) image of Pdots in aqueous solution. (C) Mechanisms of the Pdots for oxygen sensing and PDT. Reproduced with permission from Ref[23].

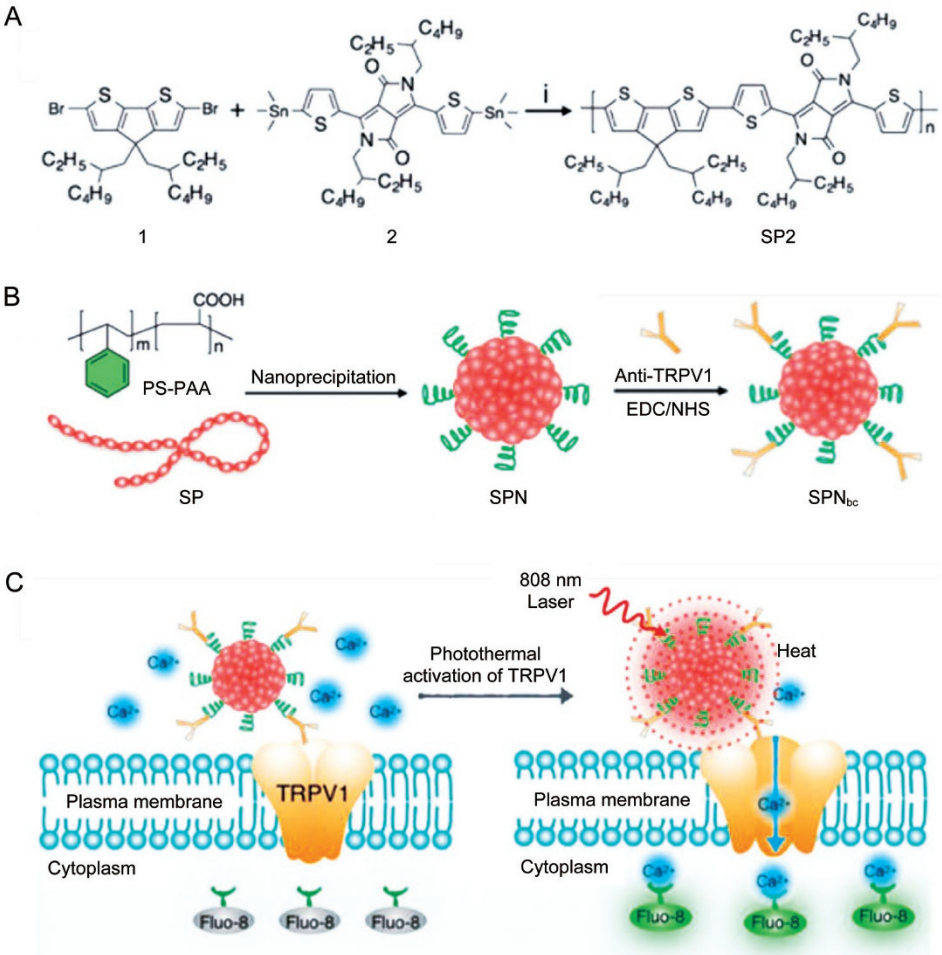


**Figure 10.** (A) Synthetic route of conjugated polymer SP2. (B) Preparation of the SPN and SPNbc with anti-TRPV1 on the surface. (C) Schematic of SPNbc-mediated photothermal activation of ion channels in neurons. Fluo-8 was used as the in real-time indicator of the intracellular concentration of calcium ions. Reproduced with permission from Ref[101].

sensing, imaging, and PDT applications[24, 86, 96–100].

Lyu *et al* found that NIR-absorbing semiconducting polymer nanoparticles (SPNs) with high photothermal conversion efficiency could control the thermo-sensitive ion channels in neurons[101] (Figure 10). The SPNs absorbed NIR laser at 808 nm with deep tissue penetration capability. Transient receptor potential cation channel subfamily V member 1 (TRPV1) is a protein widely expressed in the mammalian nervous system[102]. The surface of SPNs were functionalized with the anti-TRPV1 antibody, which targeted the temperature-sensitive ion channels (Figure 10A and 10B). When exposed to NIR laser irradiation at 808 nm, the SPNs remotely increased the local temperature, then rapidly and specifically activated the TRPV1 to gate the intracellular calcium influx of the neural cells in a reversible and safe manner (Figure 10C). The ability of the nanoparticle to activate TRPV1 was evaluated using mouse neuroblastoma/rat DRG neuron hybrid ND7/23 cells. This CPN-based photothermal approach activated neurons within milliseconds.

### CPNs for stimuli-responsive drug delivery systems

Stimuli-responsive drug delivery systems (DDSs) are promising for treating a variety of diseases through improvements in biological specificity and therapeutic efficacy[103–113]. CPN-based DDSs have been devoted to creating an on-demand drug release system via different triggers, including electrostatic repulsion, pH, enzyme, ATP, ROS, temperature, and hypoxia[10, 11]. Furthermore, CPNs provide an excellent opportunity to integrate imaging and therapeutic capability into a single delivery system, facilitating the real-time monitoring of localization of the drugs and assessment of *in vivo* therapeutic efficacy.

Yu and co-workers developed a cationic conjugated polymer core-shell nanoparticle for delivery of short interfering RNA (siRNA) and electrostatic repulsion-triggered intracellular release of the cargo[114]. The designed nanocarrier had three components: a cationic yellow-emissive conjugated polymer (BtPFN) nanoparticle as the core, an anionic siRNA attached to the core, and a sequentially electrostatically adsorbed layer

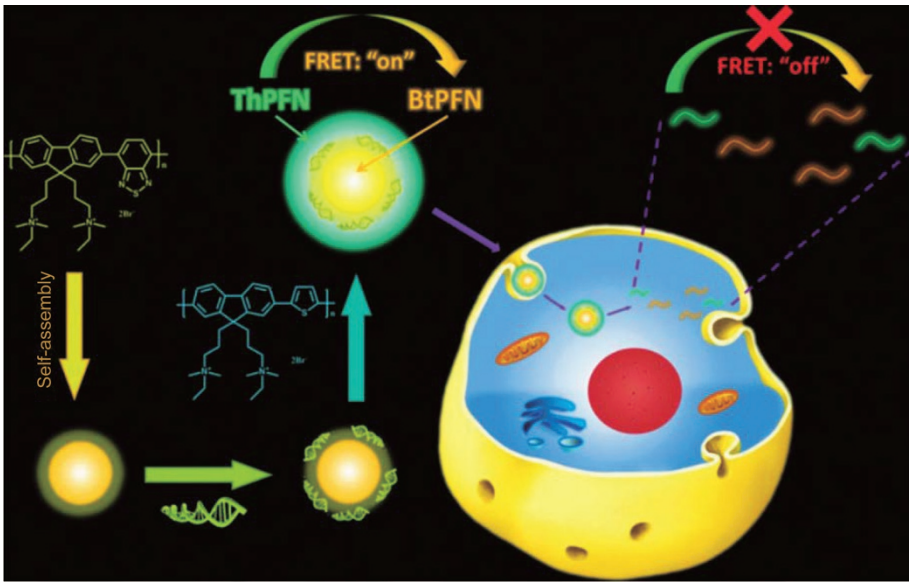


**Figure 11.** Fluorescent CPNs as siRNA nanocarriers by the sequential electrostatic assembly of siRNA and ThPFN on BtPFN nanoparticles. Reproduced with permission from Ref[114].

of a cationic green-emissive conjugated polymer (ThPFN) as the shell (Figure 11). The cationic ThPFN shell protected the delivered siRNA from ribonuclease and interacted with the negatively charged cell membranes, leading to high transfection efficiency. Owing to the large overlap in the spectra of ThPFN emission and BtPFN absorption, FRET occurred within the three-layer complexes. After uptake by the cells, siRNA was gradually released from the complexes, which was attributed to the protonation of the base groups of siRNA in acidic endosomes resulting in weakened electrostatic interactions between siRNA and the cationic polymer[115–117].

A CPN-based nanoplatform also has the potential to become a theranostic tool for imaging-guided therapy in the personalized treatment of some malignancies. Liu and co-workers also reported on CPN-based theranostic nanoplatforms (NIR NPs) for the effective delivery of siRNA *in vivo* and simultaneous real-time tracking of tumor accumulation via noninvasive NIR imaging[118] (Figure 12A). In this unique electrostatic assembly strategy[114], cationic lipid is added to afford the nanomaterials. The NIR NPs were small (~50 nm) (Figure 12B), displayed long blood circulation and high tumor accumulation, and facilitated tumor *in vivo* imaging (Figure 12C). In addition, the NIR NPs were also used for NIR imaging of sentinel lymph nodes (SLNs), which indicated that the NPs may be useful in imaging-guided location and removal of lymph nodes (Figure 12D). Immunochemical histological observation showed that the NIR NPs can efficiently silence the expression of V-Raf murine sarcoma viral oncogene homolog B (BRAF) in tumor tissues (Figure 12E). Furthermore, *in vivo* results revealed that this siRNA delivery system provided significant inhibition of tumor growth and metastasis in an orthotopic mouse model of anaplastic thyroid cancer (ATC) (Figure 12F).

Yu *et al* described a pH-responsive and NIR-emissive CPN for the simultaneous delivery and tracking of the anticancer drug doxorubicin (DOX)[119]. They utilized the CPNs to monitor the release of the anticancer drug in a non-invasive and real-time manner. *In vivo* studies showed that during degradation of the nanoparticles within a mildly acidic microenvironment at the tumor site, the NIR fluorescence intensity of the conjugated polymer decreased remarkably with the fading of FRET efficiency between the CPN and DOX. Meanwhile, the growth of the tumor was significantly inhibited. The dual-functional nanoparticles facilitated cancer therapy by monitoring drug biodistribution *in vivo*.

Inspired by the "closed-loop" design[120, 121], Chen *et al* came up with the "negative-feedback" control circuit to treat obesity[122]. Lipase is the principal enzyme responsible for hydrolysis and subsequent absorption of dietary fat[123]. They designed a lipase-sensitive conjugated polymer-based nanocarrier encapsulating orlistat, a pancreatic and gastro-intestinal lipase inhibitor[124] (Figure 13A). The nanocarriers were subject to degradation in the digestive tract because the high concentration of lipase triggered the release of the loaded orlistat. The released drug irreversibly deactivated the lipase, which in turn decreased the release speed of the drug payload, creating a negative-feedback circuit (Figure 13B). Meanwhile, orlistat reduced the gastro-intestinal absorption of fats, which finally led to a long-term reduction of body weight. Diet-induced obesity (DIO) mice were then treated by CPNs through oral gavage. The results revealed that a single dose of the nanocarrier prevented weight gain over eight days. Compared to the control group, the daily administration of the CPNs led to the lower weight of livers or fat pads, lower total cholesterol level, and smaller adipocyte size.

Qian and co-workers reported an innovative conjugated polymer-based nanocarrier capable of achieving NIR imaging

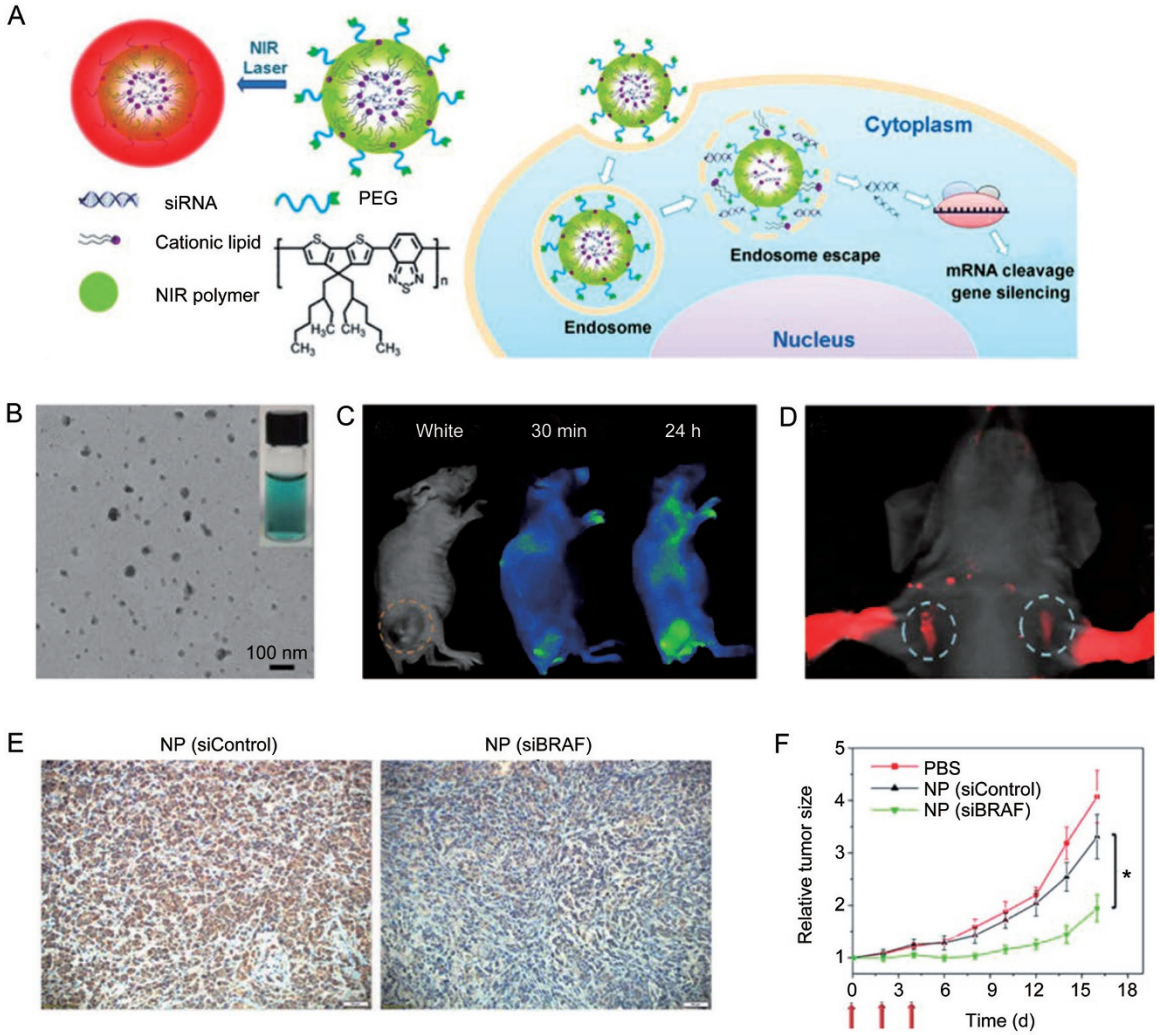


**Figure 12.** (A) Schematic of the near-infrared (NIR) polymer nanoplatforms (NPs) for siRNA delivery. (B) The TEM image and the digital picture of the NIR NPs. (C) NIR imaging. (D) Sentinel lymph node (SLN) mapping within 10 min after sc injection of NIR NPs into the forepaws. (E) Immunochemical histological observation of BRAF expression in $BRAF^{V600E}$-mutated 8505C tumor tissue after treatment with different groups: NP (siControl) or NP (siBRAF). BRAF indicates V-Raf murine sarcoma viral oncogene homolog B. (F) Tumor growth curves of PBS-, NP (siControl)-, and NP (siBRAF)-treated the mice. $^{*}P<0.05$ *vs* NP (siControl). Reproduced with permission from Ref[118].

and adenosine-5′-triphosphate (ATP)-responsive anticancer drug release[125]. Considering the distinct difference in the ATP levels between the extra- and intra-cellular milieu, CPNs were functionalized with phenylboronic acid on the surface as binding sites, which could be converted to the water-soluble polyelectrolytes in an ATP-rich environment. *In vivo* studies showed that this formulation exhibited promising capability for inhibiting tumor growth. Furthermore, the metabolism process could be evaluated by monitoring the fluorescence signal of the conjugated polymer via *in vivo* NIR imaging.

Liu and co-workers reported a ROS-activatable polyprodrug, which conjugates the DOX molecules to a polyelectrolyte via ROS-cleavable dithioketal linkers[46]. This polyprodrug system can be utilized for targeted and image-guided on-demand PDT and chemotherapy (Figure 14). To obtain biocompatibility and targetability, they also conjugated hydrophilic PEG and cyclic arginine-glycine-aspartic acid tripeptide (cRGD) to the conjugated polymer (Figure 14A). In aqueous media, the obtained polyprodrug self-assembled into nanoparticles (NPs), which exhibited both bright fluorescence for cell imaging and served as a photosensitizer to generate ROS efficiently for triggering on-demand DOX release and PDT (Figure 14B). Cell imaging and flow cytometry showed the effective light-controlled drug release. *In vitro* cytotoxicity studies confirmed enhanced cell viability inhibition for the combined therapy compared to single modality treatment.

Liu and co-workers also reported a photothermal-activatable CP nanoplatform for cancer therapy[92]. Upon a single laser irradiation, the conjugated polymer could efficiently convert the laser energy into hyperthermal energy for PTT. Moreover, the hydrophobic polymer matrix bearing many 2-diazo-1,2-naphthoquinones (DNQ) moieties could be transformed

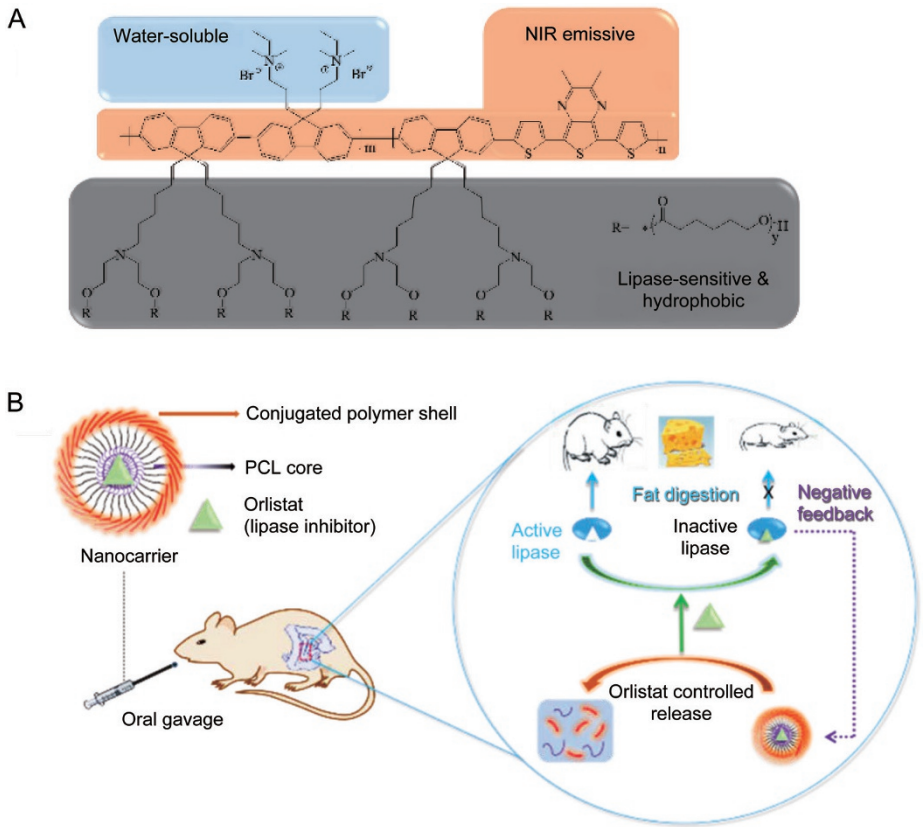


**Figure 13.** (A) Chemical structure of the conjugated polymer. (B) Schematic of lipase-sensitive conjugated polymer nanocarrier for orlistat delivery via oral gavage: orlistat release triggered by lipase, deactivation of lipase and inhibition of fat digestion, and negative feedback to control the release of the enzyme inhibitor. Reproduced with permission from Ref[122].

into a hydrophilic one simultaneously, leading to rapid drug release. The synchronous combination of PTT with chemotherapy showed a synergistic therapeutic efficiency compared to single modality treatment.

Recently, Qian *et al* designed a conjugated polymer-based nanocarrier for enhanced anticancer therapy by integrating a PDT system with a hypoxia-responsive drug delivery system[48]. This system was capable of light-induced $^1O_2$ generation and hypoxia-responsive drug release. The conjugated polymer (CP-Br) with a dithiophene-benzotriazole[126] moiety could be utilized as a visible/near-infrared light activated ROS generation source. Then, the CP-Br was further grafted with a hydrophobic hypoxia-sensitive molecule, 2-nitroimidazole (NI), to achieve hypoxia-responsive transduction. NI could be converted to hydrophilic 2-aminoimidazoles under hypoxia via a single-electron reduction catalyzed by a series of nitroreductases coupled to bio-reducing agents, such as NADPH, a plentiful coenzyme in tissues[127]. The synthesized ROS-generating and hypoxia-sensitive conjugated polymer (CP-NI) was a hydrophobic polymer. A double-emulsion-based solvent evaporation/extraction method was utilized to encapsulate DOX and form a nanoscale hypoxia-responsive vesicle (Figure 15A). When the nanocarriers accumulated at the tumor microenvironment and were irradiated, the CP-NI produced singlet oxygen ($^1O_2$), resulting in the disruption of the endo-/lysosomal membrane and the induction of cancer cell apoptosis[128]. Simultaneously, the dissolved oxygen could be rapidly consumed, resulting in a local hypoxic environment[129]. Subsequently, NI groups on the CP-NI were reduced to hydrophilic 2-aminoimidazoles under bioreductive conditions in cells, promoting the dissociation of DOX/CP-NI, and the release of cargo. The released DOX accumulated in the cell nuclei and induced DNA damage-mediated cytotoxicity[130] (Figure 15B). *In vitro* results revealed that the delivery system significantly enhanced cell cytotoxicity and apoptotic activity. Furthermore, *in vivo* experiments demonstrated that this delivery system provided more significant tumor growth inhibition compared to the PDT alone.

## Conclusions

With a host of unique properties, including highly efficient light harvesting and emitting, excellent photostability, relatively low cytotoxicity, and versatile surface modification, conjugated polymer nanomaterials have exhibited tremendous potential for diagnostics and/or therapeutic applications. Despite the advancements described in this review, there are still many challenges to be addressed. First, the quantum yield of NIR-emissive CPNs is not as high as other typical

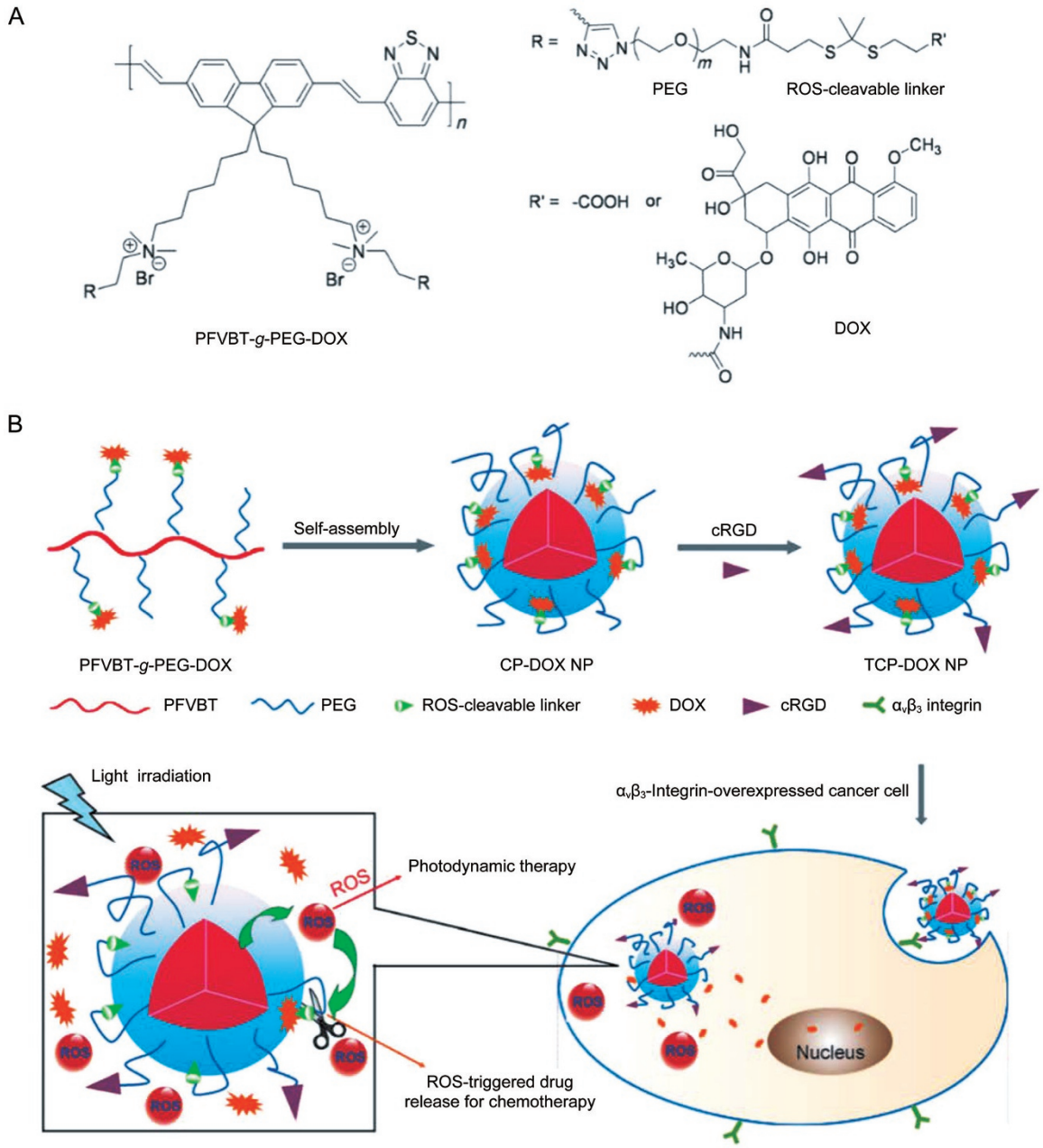


**Figure 14.** (A) Chemical structure of ROS-activatable conjugated-polyelectrolyte-based polyprodrug. (B) Self-assembled of polyprodrug nanoparticles and the light-activated ROS-responsive drug release for combination chemo-photodynamic therapy. Reproduced with permission from Ref[46].

fluorescent imaging probes[131]. Therefore, there is still a great need to overcome the current limitations and explore more potential applications. Additionally, with the unique optoelectronic characteristics, CPNs have considerable potential in the development of high-resolution fluorescence imaging technology. Second, considering the π-conjugated backbone, the metabolic processes of CPNs are not yet clear. The systemic toxicities of CPNs also require significant assessment. Third, the light-induced charge transfer could interact with other biological activities and requires further detailed study. The outcomes of these studies would further broaden the applications of CPNs in photosynthesis, optogenetics, and the transmission of neural signals.

## Acknowledgements

This work was supported by the National Natural Science Foundation of China (No 21174060) to Qun-dong SHEN, the Sloan Research Fellowship to Zhen GU, and Program A for Outstanding PhD candidate of Nanjing University to Cheng-gen QIAN. The authors also thank the China Scholarship Council for financially supporting Cheng-gen QIAN's research and living abroad.

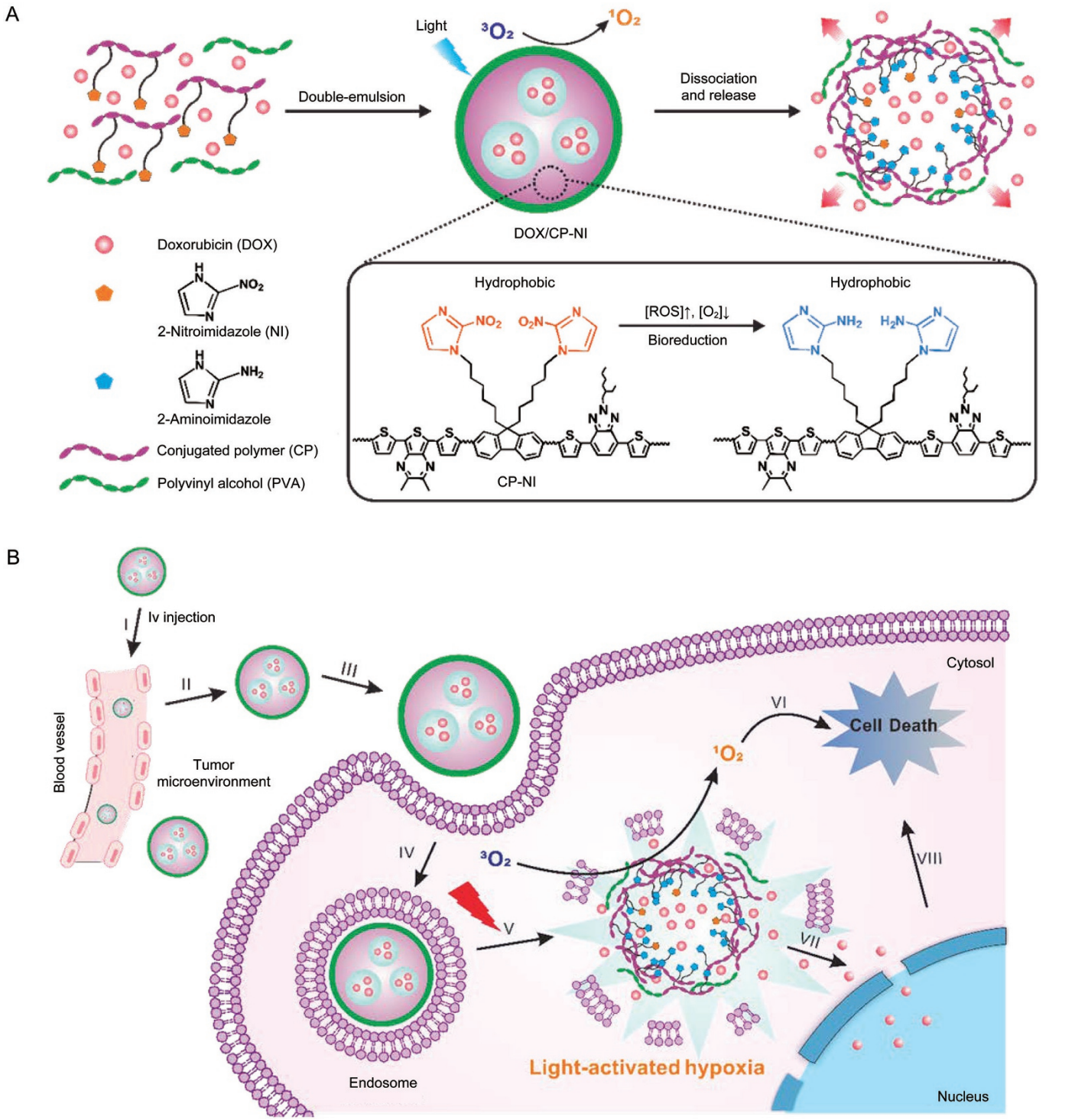


**Figure 15.** (A) Self-assembled of the light-activated hypoxia-responsive drug-delivery system. (B) Schematic of the nanocarriers for ROS generation and hypoxia-responsive drug release for enhanced synergistic anticancer efficacy. Reproduced with permission from Ref[48].

## References

1 Sariciftci NS, Smilowitz L, Heeger AJ, Wudl F. Photoinduced electron transfer from a conducting polymer to buckminsterfullerene. Science 1992; 258: 1474–6.

2 Swager TM. The molecular wire approach to sensory signal amplification. Acc Chem Res 1998; 31: 201–7.

3 Chen L, McBranch DW, Wang HL, Helgeson R, Wudl F, Whitten DG. Highly sensitive biological and chemical sensors based on reversible fluorescence quenching in a conjugated polymer. Proc Natl Acad Sci U S A 1999; 96: 12287–92.

4 Gaylord BS, Heeger AJ, Bazan GC. DNA detection using water-soluble conjugated polymers and peptide nucleic acid probes. Proc Natl

Acad Sci U S A 2002; 99: 10954–7.
5 Petros RA, DeSimone JM. Strategies in the design of nanoparticles for therapeutic applications. Nat Rev Drug Discov 2010; 9: 615–27.
6 Lammers T, Aime S, Hennink WE, Storm G, Kiessling F. Theranostic nanomedicine. Acc Chem Res 2011; 44: 1029–38.
7 Kanasty R, Dorkin JR, Vegas A, Anderson D. Delivery materials for siRNA therapeutics. Nat Mater 2013; 12: 967–77.
8 Li J, Cheng F, Huang H, Li L, Zhu JJ. Nanomaterial-based activatable imaging probes: from design to biological applications. Chem Soc Rev 2015; 44: 7855–80.
9 Mitragotri S, Anderson DG, Chen X, Chow EK, Ho D, Kabanov AV, *et al*. Accelerating the translation of nanomaterials in biomedicine. ACS Nano 2015; 9: 6644–54.
10 Lu Y, Aimetti AA, Langer R, Gu Z. Bioresponsive materials. Nat Rev Mater 2016; 1: 16075.
11 Sun W, Hu Q, Ji W, Wright G, Gu Z. Leveraging physiology for precision drug delivery. Physiol Rev 2017; 97: 189–225.
12 Gu Z, Chen XY, Shen QD, Ge HX, Xu HH. Hybrid nanocomposites of semiconductor nanoparticles and conjugated polyelectrolytes and their application as fluorescence biosensors. Polymer 2010; 51: 902–7.
13 Rose A, Zhu Z, Madigan CF, Swager TM, Bulovic V. Sensitivity gains in chemosensing by lasing action in organic polymers. Nature 2005; 434: 876–9.
14 Li K, Pan J, Feng SS, Wu AW, Pu KY, Liu Y, *et al*. Generic strategy of preparing fluorescent conjugated-polymer-loaded poly (DL-lactide-*co*-Glycolide) nanoparticles for targeted cell imaging. Adv Funct Mater 2009; 19: 3535–42.
15 Qian CG, Zhu S, Feng PJ, Chen YL, Yu JC, Tang X, *et al*. Conjugated polymer nanoparticles for fluorescence imaging and sensing of neurotransmitter dopamine in living cells and the brains of zebrafish larvae. ACS Appl Mater Interfaces 2015; 7: 18581–9.
16 Pecher J, Mecking S. Nanoparticles of conjugated polymers. Chem Rev 2010; 110: 6260–79.
17 Feng L, Zhu C, Yuan H, Liu L, Lv F, Wang S. Conjugated polymer nanoparticles: preparation, properties, functionalization and biological applications. Chem Soc Rev 2013; 42: 6620–33.
18 Wu C, Chiu DT. Highly fluorescent semiconducting polymer dots for biology and medicine. Angew Chem Int Ed Engl 2013; 52: 3086–109.
19 Pu KY, Liu B. Bioimaging: fluorescent conjugated polyelectrolytes for bioimaging. Adv Funct Mater 2011; 21: 3407–7.
20 Li K, Ding D, Huo D, Pu KY, Thao NNP, Hu Y, *et al*. Conjugated polymer based nanoparticles as dual-modal probes for targeted *in vivo* fluorescence and magnetic resonance imaging. Adv Funct Mater 2012; 22: 3107–15.
21 Xiong L, Shuhendler AJ, Rao J. Self-luminescing BRET-FRET near-infrared dots for *in vivo* lymph-node mapping and tumour imaging. Nat Commun 2012; 3: 1193.
22 Huang J, Liu Y, Qian CG, Sun MJ, Shen QD. Multicolour fluorescence cell imaging based on conjugated polymers. RSC Adv 2014; 4: 3924–8.
23 Shi H, Ma X, Zhao Q, Liu B, Qu Q, An Z, *et al*. Ultrasmall phosphorescent polymer dots for ratiometric oxygen sensing and photodynamic cancer therapy. Adv Funct Mater 2014; 24: 4823–30.
24 Zhao Q, Zhou X, Cao T, Zhang KY, Yang L, Liu S, *et al*. Fluorescent/phosphorescent dual-emissive conjugated polymer dots for hypoxia bioimaging. Chem Sci 2015; 6: 1825–31.
25 Zhang HF, Maslov K, Stoica G, Wang LV. Functional photoacoustic microscopy for high-resolution and noninvasive *in vivo* imaging. Nat Biotechnol 2006; 24: 848–51.
26 Debbage P, Jaschke W. Molecular imaging with nanoparticles: giant roles for dwarf actors. Histochem Cell Biol 2008; 130: 845–75.
27 Wang LV, Hu S. Photoacoustic tomography: *in vivo* imaging from organelles to organs. Science 2012; 335: 1458–62.
28 Janib SM, Moses AS, MacKay JA. Imaging and drug delivery using theranostic nanoparticles. Adv Drug Deliv Rev 2010; 62: 1052–63.
29 Frangioni JV. *In vivo* near-infrared fluorescence imaging. Curr Opin Chem Biol 2003; 7: 626–34.
30 Kim S, Lim YT, Soltesz EG, De Grand AM, Lee J, Nakayama A, *et al*. Near-infrared fluorescent type II quantum dots for sentinel lymph node mapping. Nat Biotechnol 2004; 22: 93–7.
31 Larson DR, Zipfel WR, Williams RM, Clark SW, Bruchez MP, Wise FW, *et al*. Water-soluble quantum dots for multiphoton fluorescence imaging *in vivo*. Science 2003; 300: 1434–6.
32 Schenke-Layland K, Riemann I, Damour O, Stock UA, König K. Two-photon microscopes and *in vivo* multiphoton tomographs — powerful diagnostic tools for tissue engineering and drug delivery. Adv Drug Deliv Rev 2006; 58: 878–96.
33 Ntziachristos V, Razansky D. Molecular imaging by means of multispectral optoacoustic tomography (MSOT). Chem Rev 2010; 110: 2783–94.
34 Kim J, Piao Y, Hyeon T. Multifunctional nanostructured materials for multimodal imaging, and simultaneous imaging and therapy. Chem Soc Rev 2009; 38: 372–90.
35 Lee DE, Koo H, Sun IC, Ryu JH, Kim K, Kwon IC. Multifunctional nanoparticles for multimodal imaging and theragnosis. Chem Soc Rev 2012; 41: 2656–72.
36 Li K, Liu B. Polymer-encapsulated organic nanoparticles for fluorescence and photoacoustic imaging. Chem Soc Rev 2014; 43: 6570–97.
37 Dolmans DE, Fukumura D, Jain RK. Photodynamic therapy for cancer. Nat Rev Cancer 2003; 3: 380–7.
38 Lovell JF, Liu TW, Chen J, Zheng G. Activatable photosensitizers for imaging and therapy. Chem Rev 2010; 110: 2839–57.
39 Cheng L, Wang C, Feng L, Yang K, Liu Z. Functional nanomaterials for phototherapies of cancer. Chem Rev 2014; 114: 10869–939.
40 Zhou Z, Song J, Nie L, Chen X. Reactive oxygen species generating systems meeting challenges of photodynamic cancer therapy. Chem Soc Rev 2016; 45: 6597–626.
41 El-Sayed IH, Huang X, El-Sayed MA. Selective laser photo-thermal therapy of epithelial carcinoma using anti-EGFR antibody conjugated gold nanoparticles. Cancer Lett 2006; 239: 129–35.
42 Huang X, El-Sayed IH, Qian W, El-Sayed MA. Cancer cell imaging and photothermal therapy in the near-infrared region by using gold nanorods. J Am Chem Soc 2006; 128: 2115–20.
43 Yang K, Zhang S, Zhang G, Sun X, Lee ST, Liu Z. Graphene in mice: ultrahigh *in vivo* tumor uptake and efficient photothermal therapy. Nano Lett 2010; 10: 3318–23.
44 Zhang Y, Song W, Geng J, Chitgupi U, Unsal H, Federizon J, *et al*. Therapeutic surfactant-stripped frozen micelles. Nat Commun 2016; 7: 11649.
45 Lu Y, Sun W, Gu Z. Stimuli-responsive nanomaterials for therapeutic protein delivery. J Control Release 2014; 194: 1–19.
46 Yuan Y, Liu J, Liu B. Conjugated-polyelectrolyte-based polyprodrug: targeted and image-guided photodynamic and chemotherapy with on-demand drug release upon irradiation with a single light source. Angew Chem Int Ed Engl 2014; 53: 7163–8.
47 Pacardo DB, Ligler FS, Gu Z. Programmable nanomedicine: synergistic and sequential drug delivery systems. Nanoscale 2015; 7: 3381–91.
48 Qian C, Yu J, Chen Y, Hu Q, Xiao X, Sun W, *et al*. Light-activated

hypoxia-responsive nanocarriers for enhanced anticancer therapy. Adv Mater 2016; 28: 3313–20.
49 Xu LG, Cheng L, Wang C, Peng R, Liu Z. Conjugated polymers for photothermal therapy of cancer. Poly Chem 2014; 5: 1573–80.
50 Stephens DJ, Allan VJ. Light microscopy techniques for live cell imaging. Science 2003; 300: 82–6.
51 Zhu C, Liu L, Yang Q, Lv F, Wang S. Water-soluble conjugated polymers for imaging, diagnosis, and therapy. Chem Rev 2012; 112: 4687–735.
52 Jin GR, Mao D, Cai PQ, Liu RR, Tomczak N, Liu J, *et al.* Conjugated polymer nanodots as ultrastable long-term trackers to understand mesenchymal stem cell therapy in skin regeneration. Adv Funct Mater 2015; 25: 4263–73.
53 Welsher K, Liu Z, Sherlock SP, Robinson JT, Chen Z, Daranciang D, *et al.* A route to brightly fluorescent carbon nanotubes for near-infrared imaging in mice. Nat Nanotechnol 2009; 4: 773–80.
54 Hong G, Lee JC, Robinson JT, Raaz U, Xie L, Huang NF, *et al.* Multifunctional *in vivo* vascular imaging using near-infrared II fluorescence. Nat Med 2012; 18: 1841–6.
55 Naczynski D, Tan M, Zevon M, Wall B, Kohl J, Kulesa A, *et al.* Rare-earth-doped biological composites as *in vivo* shortwave infrared reporters. Nat Commun 2013; 4: 2199.
56 Welsher K, Sherlock SP, Dai H. Deep-tissue anatomical imaging of mice using carbon nanotube fluorophores in the second near-infrared window. Proc Natl Acad Sci U S A 2011; 108: 8943–8.
57 Hong G, Zou Y, Antaris AL, Diao S, Wu D, Cheng K, *et al.* Ultrafast fluorescence imaging *in vivo* with conjugated polymer fluorophores in the second near-infrared window. Nat Commun 2014; 5: 4206.
58 Zhang XD, Wang H, Antaris AL, Li L, Diao S, Ma R, *et al.* Traumatic brain injury imaging in the second near-infrared window with a molecular fluorophore. Adv Mater 2016; 28: 6872–9.
59 Cahalan MD, Parker I, Wei SH, Miller MJ. Two-photon tissue imaging: seeing the immune system in a fresh light. Nat Rev Immunol 2002; 2: 872–80.
60 Helmchen F, Denk W. Deep tissue two-photon microscopy. Nat Methods 2005; 2: 932–40.
61 Denk W, Strickler JH, Webb WW. Two-photon laser scanning fluorescence microscopy. Science 1990; 248: 73–6.
62 Piston DW. Imaging living cells and tissues by two-photon excitation microscopy. Trends Cell Biol 1999; 9: 66–9.
63 Jiang H, Taranekar P, Reynolds JR, Schanze KS. Conjugated polyelectrolytes: synthesis, photophysics, and applications. Angew Chem Int Ed Engl 2009; 48: 4300–16.
64 Gao D, Agayan RR, Xu H, Philbert MA, Kopelman R. Nanoparticles for two-photon photodynamic therapy in living cells. Nano Lett 2006; 6: 2383–6.
65 Ding D, Goh CC, Feng G, Zhao Z, Liu J, Liu R, *et al.* Ultrabright organic dots with aggregation-induced emission characteristics for real-time two-photon intravital vasculature imaging. Adv Mater 2013; 25: 6083–8.
66 Gao Y, Feng G, Jiang T, Goh C, Ng L, Liu B, *et al.* Biocompatible nanoparticles based on Diketo-Pyrrolo-Pyrrole (DPP) with aggregation-induced Red/NIR emission for *in vivo* two-photon fluorescence imaging. Adv Funct Mater 2015; 25: 2857–66.
67 Li S, Shen X, Li L, Yuan P, Guan Z, Yao SQ, *et al.* Conjugated-polymer-based red-emitting nanoparticles for two-photon excitation cell imaging with high contrast. Langmuir 2014; 30: 7623–7.
68 Wang LV. Multiscale photoacoustic microscopy and computed tomography. Nat Photonics 2009; 3: 503–9.
69 Pu KY, Liu B. Fluorescent conjugated polyelectrolytes for bioimaging. Adv Funct Mater 2011; 21: 3408–23.
70 Pu K, Chattopadhyay N, Rao J. Recent advances of semiconducting polymer nanoparticles in *in vivo* molecular imaging. J Control Release 2016; 240: 312–22.
71 Pu K, Shuhendler AJ, Jokerst JV, Mei J, Gambhir SS, Bao Z, *et al.* Semiconducting polymer nanoparticles as photoacoustic molecular imaging probes in living mice. Nat Nanotechnol 2014; 9: 233–9.
72 Lyu Y, Fang Y, Miao Q, Zhen X, Ding D, Pu K. Intraparticle molecular orbital engineering of semiconducting polymer nanoparticles as amplified theranostics for *in vivo* photoacoustic imaging and photothermal therapy. ACS Nano 2016; 10: 4472–81.
73 Fan Q, Cheng K, Yang Z, Zhang R, Yang M, Hu X, *et al.* Perylene-diimide-based nanoparticles as highly efficient photoacoustic agents for deep brain tumor imaging in living mice. Adv Mater 2015; 27: 843–7.
74 Sun B, Zhang Y, Gu KJ, Shen QD, Yang Y, Song H. Layer-by-layer assembly of conjugated polyelectrolytes on magnetic nanoparticle surfaces. Langmuir 2009; 25: 5969–73.
75 Sun B, Sun MJ, Gu Z, Shen QD, Jiang SJ, Xu Y, *et al.* Conjugated polymer fluorescence probe for intracellular imaging of magnetic nanoparticles. Macromolecules 2010; 43: 10348–54.
76 Liu Y, Huang J, Sun MJ, Yu JC, Chen YL, Zhang YQ, *et al*. A fluorescence-Raman dual-imaging platform based on complexes of conjugated polymers and carbon nanotubes. Nanoscale 2014; 6: 1480–9.
77 Fan Q, Cheng K, Hu X, Ma X, Zhang R, Yang M, *et al.* Transferring biomarker into molecular probe: melanin nanoparticle as a naturally active platform for multimodality imaging. J Am Chem Soc 2014; 136: 15185–94.
78 Cheng Z, Mahmood A, Li H, Davison A, Jones AG. [$^{99m}$TcOAADT]-$(CH_2)_2$-$NEt_2$: a potential small-molecule single-photon emission computed tomography probe for imaging metastatic melanoma. Cancer Res 2005; 65: 4979–86.
79 Ren G, Miao Z, Liu H, Jiang L, Limpa-Amara N, Mahmood A, *et al.* Melanin-targeted preclinical PET imaging of melanoma metastasis. J Nucl Med 2009; 50: 1692–9.
80 Zhang R, Fan Q, Yang M, Cheng K, Lu X, Zhang L, *et al.* Engineering melanin nanoparticles as an efficient drug-delivery system for imaging-guided chemotherapy. Adv Mater 2015; 27: 5063–9.
81 Wang X, Li S, Zhang P, Lv F, Liu L, Li L, *et al.* An optical nanoruler based on a conjugated polymer-silver nanoprism pair for label-free protein detection. Adv Mater 2015; 27: 6040–5.
82 Yuan H, Qi J, Xing C, An H, Niu R, Zhan Y, *et al.* Graphene-oxide-conjugated polymer hybrid materials for calmodulin sensing by using FRET strategy. Adv Funct Mater 2015; 25: 4412–8.
83 Yuan H, Wang B, Lv F, Liu L, Wang S. Conjugated-polymer-based energy-transfer systems for antimicrobial and anticancer applications. Adv Mater 2014; 26: 6978–82.
84 Corbitt TS, Sommer JR, Chemburu S, Ogawa K, Ista LK, Lopez GP, *et al.* Conjugated polyelectrolyte capsules: light-activated antimicrobial micro “roach motels”. ACS Appl Mater Interfaces 2008; 1: 48–52.
85 Zhu C, Yang Q, Lv F, Liu L, Wang S. Conjugated polymer-coated bacteria for multimodal intracellular and extracellular anticancer activity. Adv Mater 2013; 25: 1203–8.
86 Zhou X, Liang H, Jiang P, Zhang KY, Liu S, Yang T, *et al*. Multifunctional phosphorescent conjugated polymer dots for hypoxia imaging and photodynamic therapy of cancer cells. Adv Sci (Weinh) 2015; 3: 1500155.
87 Geng J, Sun C, Liu J, Liao LD, Yuan Y, Thakor N, *et al.* Biocompatible conjugated polymer nanoparticles for efficient photothermal tumor therapy. Small 2015; 11: 1603–10.
88 Yuan Y, Liu B. Self-assembled nanoparticles based on PEGylated

conjugated polyelectrolyte and drug molecules for image-guided drug delivery and photodynamic therapy. ACS Appl Mater Interfaces 2014; 6: 14903–10.
89 Feng GX, Liu J, Geng JL, Liu B. Conjugated polymer microparticles for selective cancer cell image-guided photothermal therapy. J Mater Chem B 2015; 3: 1135–41.
90 Wu WB, Feng GX, Xu SD, Liu B. A Photostable far-red/near-infrared conjugated polymer photosensitizer with aggregation-induced emission for image-guided cancer cell ablation. Macromolecules 2016; 49: 5017–25.
91 Yuan Y, Min Y, Hu Q, Xing B, Liu B. NIR photoregulated chemo- and photodynamic cancer therapy based on conjugated polyelectrolyte-drug conjugate encapsulated upconversion nanoparticles. Nanoscale 2014; 6: 11259–72.
92 Yuan Y, Wang Z, Cai P, Liu J, Liao LD, Hong M, *et al.* Conjugated polymer and drug co-encapsulated nanoparticles for chemo- and photo-thermal combination therapy with two-photon regulated fast drug release. Nanoscale 2015; 7: 3067–76.
93 Guo B, Feng G, Manghnani PN, Cai X, Liu J, Wu W, *et al.* A porphyrin-based conjugated polymer for highly efficient *in vitro* and *in vivo* photothermal therapy. Small 2016; 12: 6243–54.
94 You Y, Lee S, Kim T, Ohkubo K, Chae WS, Fukuzumi S, *et al.* Phosphorescent sensor for biological mobile zinc. J Am Chem Soc 2011; 133: 18328–42.
95 Shi C, Sun H, Tang X, Lv W, Yan H, Zhao Q, *et al.* Variable photophysical properties of phosphorescent iridium (III) complexes triggered by closo- and nido-carborane substitution. Angew Chem Int Ed Engl 2013; 52: 13434–8.
96 Shi H, Sun H, Yang H, Liu S, Jenkins G, Feng W, *et al.* Cationic polyfluorenes with phosphorescent iridium (III) complexes for time-resolved luminescent biosensing and fluorescence lifetime imaging. Adv Funct Mater 2013; 23: 3268–76.
97 Lv W, Yang T, Yu Q, Zhao Q, Zhang KY, Liang H, *et al.* A phosphorescent iridium (III) complex-modified nanoprobe for hypoxia bioimaging via time-resolved luminescence microscopy. Adv Sci (Weinh) 2015; 2: 1500107.
98 Li J, Yuan Y, Zeng G, Li X, Yang Z, Li X, *et al.* A water-soluble conjugated polymer with azobenzol side chains based on "turn-on" effect for hypoxic cell imaging. Poly Chem 2016; 7: 6890–4.
99 Lv W, Zhang Z, Zhang KY, Yang H, Liu S, Xu A, *et al.* A mitochondria-targeted photosensitizer showing improved photodynamic therapy effects under hypoxia. Angew Chem Int Ed Engl 2016; 128: 10101–5.
100 Zhen X, Zhang C, Xie C, Miao Q, Lim KL, Pu K. Intraparticle energy level alignment of semiconducting polymer nanoparticles to amplify chemiluminescence for ultrasensitive *in vivo* imaging of reactive oxygen species. ACS Nano 2016; 10: 6400–9.
101 Lyu Y, Xie C, Chechetka SA, Miyako E, Pu K. Semiconducting polymer nanobioconjugates for targeted photothermal activation of neurons. J Am Chem Soc 2016; 138: 9049–52.
102 Tominaga M, Caterina MJ, Malmberg AB, Rosen TA, Gilbert H, Skinner K, *et al.* The cloned capsaicin receptor integrates multiple pain-producing stimuli. Neuron 1998; 21: 531–43.
103 Sarikaya M, Tamerler C, Jen AK, Schulten K, Baneyx F. Molecular biomimetics: nanotechnology through biology. Nat Mater 2003; 2: 577–85.
104 Yoo JW, Irvine DJ, Discher DE, Mitragotri S. Bio-inspired, bioengineered and biomimetic drug delivery carriers. Nat Rev Drug Discov 2011; 10: 521–35.
105 Mo R, Jiang T, DiSanto R, Tai W, Gu Z. ATP-triggered anticancer drug delivery. Nat Commun 2014; 5: 3364.
106 Hu Q, Sun W, Qian C, Wang C, Bomba HN, Gu Z. Anticancer platelet-mimicking nanovehicles. Adv Mater 2015; 27: 7043–50.
107 Wang H, Jiang Y, Peng H, Chen Y, Zhu P, Huang Y. Recent progress in microRNA delivery for cancer therapy by non-viral synthetic vectors. Adv Drug Deliv Rev 2015; 81: 142–60.
108 Wang Q, Cheng H, Peng H, Zhou H, Li PY, Langer R. Non-genetic engineering of cells for drug delivery and cell-based therapy. Adv Drug Deliv Rev 2015; 91: 125–40.
109 Su J, Sun H, Meng Q, Yin Q, Tang S, Zhang P, *et al.* Long circulation red-blood-cell-mimetic nanoparticles with peptide-enhanced tumor penetration for simultaneously inhibiting growth and lung metastasis of breast cancer. Adv Funct Mater 2016; 26: 1243–52.
110 Su J, Sun H, Meng Q, Yin Q, Zhang P, Zhang Z, *et al.* Bioinspired nanoparticles with nir-controlled drug release for synergetic chemophotothermal therapy of metastatic breast cancer. Adv Funct Mater 2016; 26: 7495–506.
111 Sun H, Su J, Meng Q, Yin Q, Chen L, Gu W, *et al.* Cancer-cell-biomimetic nanoparticles for targeted therapy of homotypic tumors. Adv Mater 2016; 28: 9581–8.
112 Wang D, Wang T, Liu J, Yu H, Jiao S, Feng B, *et al.* Acid-activatable versatile micelleplexes for PD-L1 blockade-enhanced cancer photodynamic immunotherapy. Nano Lett 2016; 16: 5503–13.
113 Wang T, Wang D, Yu H, Wang M, Liu J, Feng B, *et al.* Intracellularly acid-switchable multifunctional micelles for combinational photo/chemotherapy of the drug-resistant tumor. ACS Nano 2016; 10: 3496–508.
114 Yu JC, Zhu S, Feng PJ, Qian CG, Huang J, Sun MJ, *et al.* Cationic fluorescent polymer core-shell nanoparticles for encapsulation, delivery, and non-invasively tracking the intracellular release of siRNA. Chem Commun (Camb) 2015; 51: 2976–9.
115 Wang X, He F, Li L, Wang H, Yan R, Li L. Conjugated oligomer-based fluorescent nanoparticles as functional nanocarriers for nucleic acids delivery. ACS Appl Mater Interfaces 2013; 5: 5700–8.
116 Jiang R, Lu X, Yang M, Deng W, Fan Q, Huang W. Monodispersed brush-like conjugated polyelectrolyte nanoparticles with efficient and visualized siRNA delivery for gene silencing. Biomacromolecules 2013; 14: 3643–52.
117 Qiu F, Wang D, Zhu Q, Zhu L, Tong G, Lu Y, *et al.* Real-time monitoring of anticancer drug release with highly fluorescent star-conjugated copolymer as a drug carrier. Biomacromolecules 2014; 15: 1355–64.
118 Liu Y, Gunda V, Zhu X, Xu X, Wu J, Askhatova D, *et al.* Theranostic near-infrared fluorescent nanoplatform for imaging and systemic siRNA delivery to metastatic anaplastic thyroid cancer. Proc Natl Acad Sci U S A 2016; 113: 7750–5.
119 Yu JC, Chen YL, Zhang YQ, Yao XK, Qian CG, Huang J, *et al.* pH-Responsive and near-infrared-emissive polymer nanoparticles for simultaneous delivery, release, and fluorescence tracking of doxorubicin *in vivo*. Chem Commun (Camb) 2014; 50: 4699–702.
120 Mo R, Jiang T, Di J, Tai W, Gu Z. Emerging micro- and nanotechnology based synthetic approaches for insulin delivery. Chem Soc Rev 2014; 43: 3595–629.
121 Veiseh O, Tang BC, Whitehead KA, Anderson DG, Langer R. Managing diabetes withnanomedicine: challenges and opportunities. Nat Rev Drug Discov 2015; 14: 45–57.
122 Chen YL, Zhu S, Zhang L, Feng PJ, Yao XK, Qian CG, *et al.* Smart conjugated polymer nanocarrier for healthy weight loss by negative feedback regulation of lipase activity. Nanoscale 2016; 8: 3368–75.
123 de la Garza AL, Milagro FI, Boque N, Campión J, Martínez JA. Natural inhibitors of pancreatic lipase as new players in obesity treatment. Planta Med 2011; 77: 773–85.
124 Chanoine JP, Hampl S, Jensen C, Boldrin M, Hauptman J. Effect of

orlistat on weight and body composition in obese adolescents: a randomized controlled trial. JAMA 2005; 293: 2873–83.
125 Qian C, Chen Y, Zhu S, Yu J, Zhang L, Feng P, *et al.* ATP-responsive and near-infrared-emissive nanocarriers for anticancer drug delivery and real-time imaging. Theranostics 2016; 6: 1053–64.
126 Patel DG, Feng F, Ohnishi YY, Abboud KA, Hirata S, Schanze KS, *et al.* It takes more than an imine: the role of the central atom on the electron-accepting ability of benzotriazole and benzothiadiazole oligomers. J Am Chem Soc 2012; 134: 2599–612.
127 Nunn A, Linder K, Strauss HW. Nitroimidazoles and imaging hypoxia. Eur J Nucl Med 1995; 22: 265–80.
128 Hogset A, Prasmickaite L, Selbo PK, Hellum M, Engesaeter BO, Bonsted A, *et al.* Photochemical internalisation in drug and gene delivery. Adv Drug Deliv Rev 2004; 56: 95–115.
129 Mitchell JB, McPherson S, DeGraff W, Gamson J, Zabell A, Russo A. Oxygen dependence of hematoporphyrin derivative-induced photoinactivation of Chinese hamster cells. Cancer Res 1985; 45: 2008–11.
130 Tewey KM, Rowe TC, Yang L, Halligan BD, Liu LF. Adriamycin-induced DNA damage mediated by mammalian DNA topoisomerase II. Science 1984; 226: 466–8.
131 Huang H, Lovell JF. Advanced functional nanomaterials for theranostics. Adv Funct Mater 2017; 27: 1603524.

**This work is licensed under the Creative Commons Attribution-NonCommercial-No Derivative Works 3.0 Unported License. To view a copy of this license, visit http://creativecommons.org/licenses/by-nc-nd/3.0/**

**© The Author(s) 2017**